A Geometrical Perspective on Localization

Stefan O. Dulman
University of Twente
The Netherlands
s.o.dulman@utwente.nl

Aline Baggio
Delft University of Technology
The Netherlands
a.baggio@ewi.tudelft.nl

Paul J.M. Havinga
Ambient Systems B.V.
The Netherlands
havinga@ambient-systems.net

Koen G. Langendoen
Delft University of Technology
The Netherlands
k.g.langendoen@tudelft.nl

ABSTRACT

A large number of localization algorithms for wireless sensor networks (WSNs) are evaluated against the Cramer-Rao Bound (CRB) as an indicator of how good the algorithm performs. The CRB defines the lower bound on the precision of an unbiased localization estimator. The CRB concept, borrowed from GPS localization, however, does not translate well to WSNs. In this paper, we show in which cases the CRB fails to capture troublesome anchor configurations leading to erroneous lower bounds. We continue with a study on the geometrical configurations of anchors favorable to localization algorithms. We conclude by proposing a metric to characterize the stability of the geometry of a certain anchor topology. Future work will address the combination of geometry and statistical metrics with the goal of obtaining a clear image on localization algorithms boundaries.

Categories and Subject Descriptors

C.2.4 [**Computer Communication Networks**]: Distributed Systems—*Distributed applications*

General Terms

Algorithms, design, theory

1. INTRODUCTION

Acquiring position information in ad-hoc networks and in particular wireless sensors networks (WSNs) received a lot of attention in the past years. Survey works, such as [1, 2], show a large number of techniques/algorithms that can be used to solve the localization problem. The techniques used are often borrowed from other fields of science and modified to fit the context of wireless sensor networks [3–5]. In order for results established in other fields of science to hold for the problem at hand, particular care must be taken to ensure that the assumptions are still valid. Even the slightest mismatch in the underlying assumptions could render the well-known techniques useless and lead to wrong results.

In this paper, we start by addressing the usage of *lateration* [6] and the associated *Cramer-Rao Bound* (CRB) [3], concepts borrowed from GPS localization [7]. Via a series of counter-examples, we show how these concepts fail to deliver the expected results when applied to the field of WSNs. We aim at bringing forward the idea that a foundation based on geometrical considerations – rather than estimation theory – should be employed when studying the basic mechanisms and boundaries for localization in WSNs.

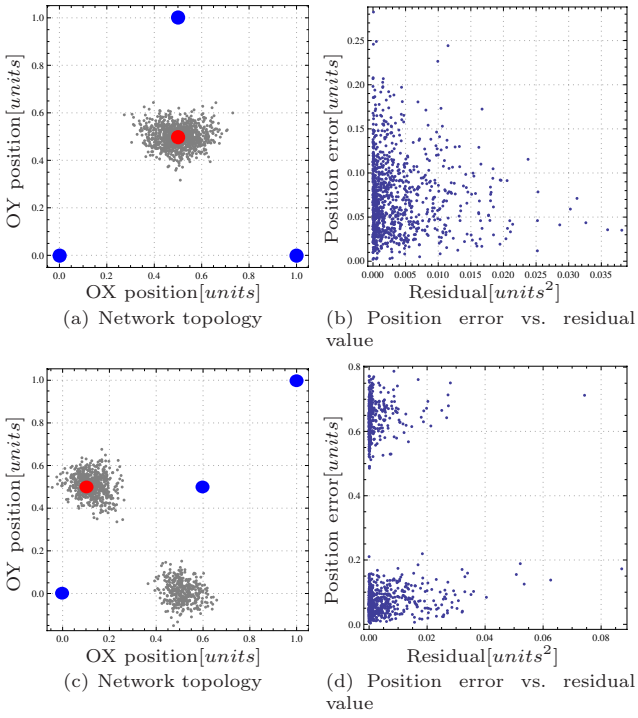

(a) Network topology (b) Position error vs. residual value

(c) Network topology (d) Position error vs. residual value

Figure 1: Lateration in the presence of noise.

MELT'08, September 19, 2008, San Francisco, California, USA.

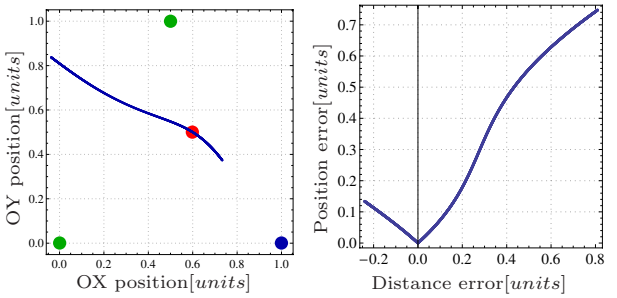

(a) Computed position trajectory (b) Position errors vs. distance error

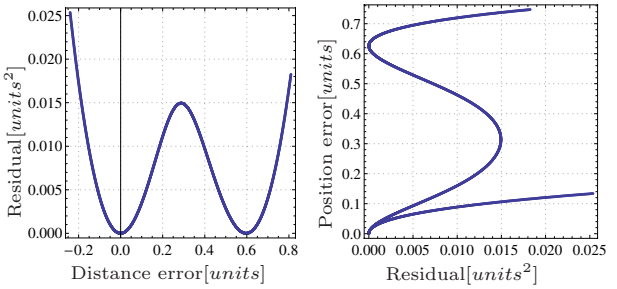

(c) Residual vs. distance error (d) Position error vs. residual

Figure 2: Lateration behavior for "regular" anchor setup.

The paper continues with an analysis of the setups involving three anchors in order to grasp the underlying geometrical localization mechanisms. We basically decouple the localization problem from estimation theory, showing that there is at least one intermediate step (involving geometry only) when computing the bounds for achievable accuracies. Based on this analysis, we introduce a metric to characterize the stability of a given setup. We use this metric to decide what is the best placement of a set of anchors in a static configuration, and plan to use it in future work to derive accurate bounds on localization accuracy.

2. THE LOCALIZATION PROBLEM

Let the position of a node in the 2D plane be written as z. The position error is defined as the Euclidean distance between the real (z) and estimated position ($\tilde{z}$) of a node, $e_i = \|z, \tilde{z}\|$. We call an *anchor* a node that acquired *exact* position information (anchor i has position a_i). A node without knowledge of its position is simply called *node*.

Assume a scenario with three anchors (blue circles in Fig. 1(a)) and a node positioned in the central area (red circle). Assuming the exact distances $\overline{d}_i$ between the node and anchors are known, the node is able to infer its position $\tilde{z}$ by intersecting the three circles centered at a_i with radii $\overline{d}_i$. If errors are added to the distance estimates, simulating measured distances d_i, no position in the 2D plane is likely to satisfy the distance constraints. Solving the localization problem then takes the form of choosing the estimated position that minimizes a certain metric. Lateration [6] is one of the most popular techniques and works as follows:

$$\tilde{z} = \arg_{\tilde{z}} \min \sum_{i=1}^{n} \omega_i \left(d_i - \tilde{d}_i \right)^2 \qquad (1)$$

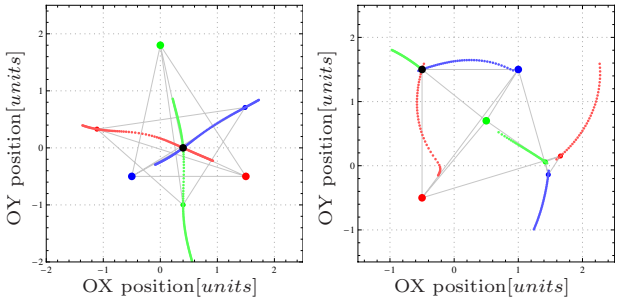

(a) Non-collinear anchor topology (b) Collinear anchor topology

Figure 3: Lateration behavior (decomposed noise components).

where $\tilde{d}_i$ are the distances between the computed position and the anchors, and ω_i a set of weights. When varying the noise in the measured distances and using equal weights, we obtain a cloud of estimated positions as shown in Fig. 1(a) in gray.

Tracing back the lateration technique we come across the concept of Cramer-Rao Bound applied to the localization problem [3]. CRB defines the lower bound on the precision of a localization estimator. The articles [3, 8, 9] solve the localization problem step-wise as follows:

a. Basic concept: known noise distributions are applied to distance measurements;

b. Theoretical step: determine CRB to obtain an idea of the achievable accuracy of unbiased position estimators;

c. Algorithm: from the formulation of CRB determine the metric to be minimized in order to obtain a position (e.g. using the lateration procedure);

d. Post processing: use coefficients such as Geometric Dilution of Precision [10] (GDOP) to correct issues not captured by the estimation theory (such as the geometry of anchor deployment).

It is *assumed* that minimizing the sums in the lateration equation leads to better position estimates. In some works the *residual value*, i.e. the minimum value for the sum, serves as an indicator on how good the algorithm performs. In Fig. 1(b), we plot the residual value versus the position error for each of the gray points in Fig. 1(a). We expected a curve passing through the origin to validate the assumption that a residual of 0 corresponds to a position error of 0. The results in Fig. 1(b) show that position error and residual value are not correlated as assumed.

In Fig. 1(c) we consider the same problem, but we moved the anchors to an almost-collinear situation. The localization algorithm does not have enough information to decide on which side of the line determined by the anchors the final position lies, so it outputs results in two clusters (one centered in the true location of the node and one in its symmetrical position with respect to the anchors line). This uncertainty is reflected in the graph of position error versus residual as well (see Fig. 1(d)). This figure shows that minimizing for the residual is not sufficient to guarantee a certain localization error.

In the following, we analyze the sources of this "flipping" uncertainty. We couple it with the inconsistencies we notice in the CRB mechanism. Working towards a solution we propose a metric to characterize it.

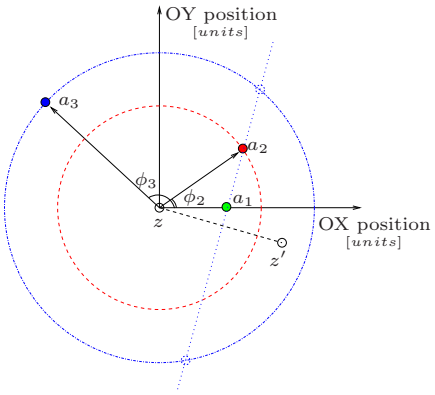

Figure 4: Circular deployment of anchors.

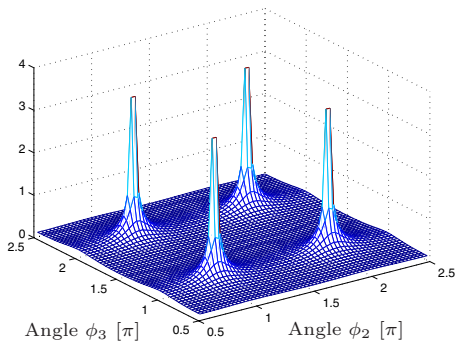

Figure 5: Cramer-Rao Bound.

3. RESIDUAL VALUE BEHAVIOR

Considering the same anchor scenario as in Fig. 1(a) and a node placed at coordinates $z = (0.6; 0.5)$ (red dot in Fig. 2(a)), we performed the following experiment: we kept the distances to two anchors constant and equal to the real distances (no noise) and only varied the distance towards the bottom-right anchor from Fig. 2(a). The blue line in Fig. 2(a) shows the set of resulting positions computed by the lateration procedure. Fig. 2(b) shows the position error versus the induced distance error. For a distance error of 0 – when the true distance is fed to the algorithm – the real position is returned. In other cases as expected, the larger the distance error is, the larger the position error becomes. Fig. 2(c) shows the value of the residual versus the induced distance error. The residual function exhibits two local minima: one corresponding to the real position (distance error equals zero) and one corresponding to the symmetrical position of the node with respect to the first two anchors (in green in Fig. 2(a)).

Fig. 2(d) shows the position error versus the residual value. This nonlinear graph shows two curves passing through the origin. The curves can be explained by the fact that in the residual expression the influence of the distance error enters always as a squared factor. Underestimating a distance or overestimating it leads to different behavior in the lateration procedure (as shown in Fig. 2(b)). This leads to the semiplane $x \in (-\infty, 0)$ being folded over the semiplane $x \in (0, \infty)$. The zigzag shape of the upper curve is a direct consequence of the residual shape in Fig. 2(c).

Fig. 3(a) shows a set of similar experiments. The three anchors (the large green, red and blue dots) are deployed around the node (black dot in middle of the triangle). We keep the distance towards two anchors equal to the real value and vary the distance towards the third anchor. The colored lines show the trajectories of the positions offered by lateration (e.g. the red dotted line shows the positions when only the distance towards the red anchor was varied). It is easy to notice that every of these trajectories include the actual position of the point and its symmetrical position with respect to the line determined by the anchors to which the distances were kept constant (represented as a smaller colored dot).

Non linearity is not the only problem at hand: discontinuities occur as well in the case of specific anchor topologies. The clustered results in Fig. 1(c) correspond to discontinuities in the trajectories offered by the lateration procedure. In Fig. 3(b) we chose a set of almost collinear anchors (big red, blue and green dots around the first diagonal). The node is placed at $z = (-0.2, 0.8)$ (black dot). The symmetrical positions of the node with respect to the lines determined by the distinct pairs of two anchors are shown as small colored dots. We keep the distances towards two anchors constant and vary the distance towards the third – the colored lines show the trajectories output by lateration. The trajectories present discontinuities – the computed position is "jumping" from one cluster to another. As expected, the trajectories contain the true position of the node and its symmetrical positions.

4. CRAMER-RAO BOUND IN LOCALIZATION

We repeated the experiment described in [9] to study the behavior of CRB (see Fig. 4). Assume three anchors a_i and a node z placed at the origin of the system of coordinates. The anchor a_1 is fixed and a_2 and a_3 are rotating around z, while maintaining the same distance towards z. In Fig. 4, the red and blue circles represent their trajectories. The goal is to compute the CRB for various angles ϕ_2 and ϕ_3 that a_2 and a_3 make with the horizontal axis in order to capture the effects of anchor geometry on localization error.

The results of this experiment are presented in Fig. 5. The axes OX and OY represent the angles ϕ_2 and ϕ_3 and are graded directly in π. The spikes, rising to $+\infty$, represent discontinuities in CRB (the axis OZ was cropped). For improved clarity, we shifted the axes with 0.5π to clearly show the four discontinuities and we represented CRB rather than 1/CRB [9]. CRB shows discontinuities in the cases where collinearity occurs, that is with the pairs of angles $(\phi_2, \phi_3) \in \{(\pi, \pi), (\pi, 2\pi), (2\pi, \pi), (2\pi, 2\pi)\}$.

There is a subtlety not described in [9]: the collinearity situation for which the CRB goes to infinity involves *the node as well* and not only the anchors. Although the findings we cited above seem intuitively correct, *they are false*. In the case of three collinear anchors in the 2D plane shown as a blue dotted line in Fig. 4 and given the distances between the node and the anchors $\overline{d}_i$, there is an uncertainty on which side of the line the node resides: at z or at its mirrored position z'. This uncertainty is not infinite. We define as a metric the *flipping uncertainty* equal to $\|z, z'\|$. The flipping uncertainty goes to zero when the node gets very close to the line determined by the collinear anchors. This implies that

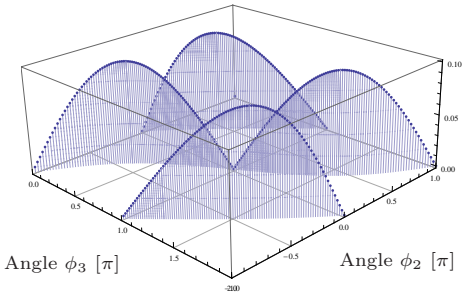

Figure 6: Flipping uncertainty.

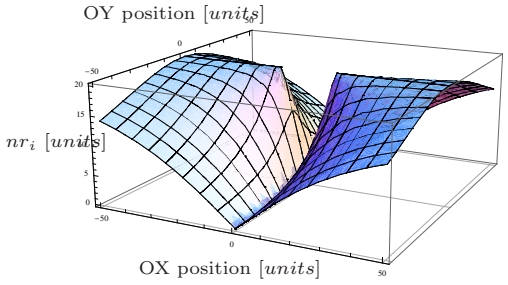

Figure 7: Noise-resilience metric over the 2D plane; the unknown node is located at (-10,0).

the only case in which a node can compute a position given a set of collinear anchors is when the node resides on the *same line* as the anchors. This contradicts the insight given by CRB.

Fig. 4 allows us to make a second important observation. For every position of a_2, there exist two possible positions in which the line determined by a_1 and a_2 intersects the trajectory of a_3. This means that for every position a_2, there exist two possibilities to place a_3 such that all three anchors are collinear. The relationship between a_1, a_2 and a_3 basically reduces to the intersection of the line (a_1, a_2) with the circle centered at z having radius $\|z, a_3\|$. Graphically the result is presented in Fig. 6. A point is placed in this picture for each situation in which the angles ϕ_2 and ϕ_3 lead to a collinear situation for the three anchors. The OZ coordinate measures the flipping uncertainty. Although Fig. 6 might look similar to Fig. 5, attention should be paid to the values on the OX and OY axis – for the points where CRB goes to infinity, the flipping uncertainty is actually 0.

The last two observations lead to the conclusion that CRB does not indicate all the troublesome anchor configurations. Worse than that, it indicates infinite uncertainty in the only situations in which positions can be computed, that is when all the anchors and the node are collinear.

As a final remark on CRB, it is worth noting that it gives a boundary on the *variance* rather than on the *mean value* of an unbiased estimator. This topic has been previously addressed as *accuracy versus precision* [11].

Previous work proposing CRB as a mechanism to determine the uncertainty of position computation shows that under certain assumptions the effects of anchors geometry can be computed as a separate coefficient, known as GDOP [7]. The expression of GDOP is actually directly derived from the expression of CRB under the following simplifying assumptions: the parameters of distance estimates (mean and variance) are considered equal thus the final formula takes only angles into account. Neither of these simplifications holds in sensor networks as opposed to a satellite system – mean values of distances of a node towards various anchors can be of different orders of magnitude and the variances are proportional to the actual distances. Furthermore, as CRB fails grasping the characteristics of the underlying geometric setup, GDOP is of little use in our case. We conclude that while it makes sense to use CRB in the context of GPS where the distances between a node and the anchors are very large and the amount of error on the distances is assumed insignificant, the method cannot be applied to WSNs.

5. A NOISE-RESILIENCE METRIC

In this section we explore the problem of placement of anchors around a node in the 2D case when distance measurements to three anchors are available.

We start with the following question: given the position of a node (z) and of two anchors (a_1, a_2) where should the third anchor (a_3) be placed such that the localization procedure provides good results?

Since the positions of the node z and anchors a_1 and a_2 are fixed, and measured distances d_1 and d_2 are not dependent on the position of a_3, we focus our reasoning on the effects that d_3 has on localization. The example from Fig. 3 demonstrates that when varying the amount of noise on one distance estimate, the resulting set of positions lies on a curve containing the true position of the node (z) and its reflected position z' with respect to the line defined by the other two anchors. Let $\overline{d}_3'$ be the real distance between a_3 and z'.

In the case that $\overline{d}_3$ and $\overline{d}_3'$ are almost equal, a little amount of measurement noise can lead to a computed position close to the reflected point z' rather than z. Intuitively, this is to be avoided as it is preferred to have a localization algorithm output one cluster of positions (see Fig. 1(a)) rather than two or more clusters (see Fig. 1(c)). The case $\overline{d}_3$ equals $\overline{d}_3'$ happens when a_1, a_2 and a_3 are collinear – thus this is indeed the worst case scenario.

In case $\overline{d}_3$ and $\overline{d}_3'$ are not equal, the difference between the two values is important. Feeding $\overline{d}_3$ in the lateration algorithm will lead to z as the computed position – while feeding $\overline{d}_3'$ leads to z'. The transition or "jump" between the two positions (as seen in Fig. 3) happens somewhere in between the two values. The larger the difference between the two values, the larger the threshold is when flipping occurs. Thus, the larger the difference between the two values, the larger the amount of noise one can tolerate to $\overline{d}_3$ such that the computed position remains in a cluster around z.

We define a *noise-resilience* metric nr_i for placing the anchor i with respect to the two other anchors as the absolute value of the difference between $\overline{d}_i$ and $\overline{d}_i'$: $nr_i(z) = |\|z, a_i\| - \|z', a_i\||$. Note that this noise-resilience metric takes into account the reflected position of the node with respect to the line determined by the other two anchors. As such the exact position of these anchors can be abstracted away; only the line determined by them is important. In order to understand the mechanism behind the noise-resilience

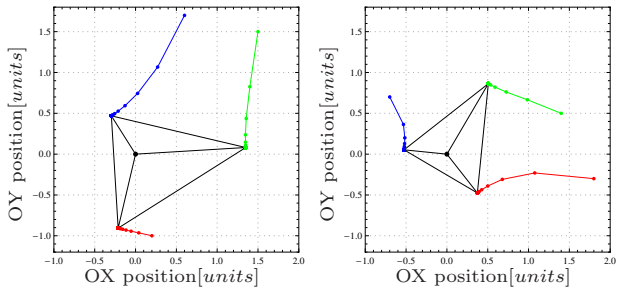

(a) Initial positions – example 1 (b) Initial positions – example 2

Figure 8: Anchor placement around one node.

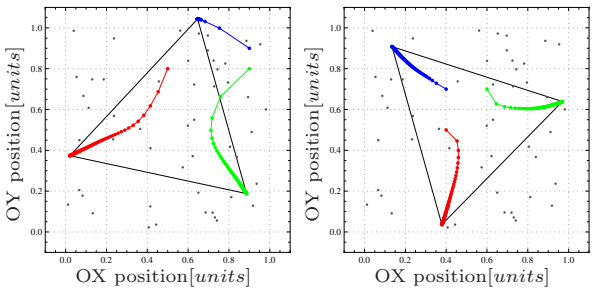

(a) Initial positions - example 1 (b) Initial positions - example 2

Figure 9: Anchor placement in a given area.

metric, we performed the following experiment: we assume that a_1 and a_2 are placed somewhere on the OY axis, the node is placed on the OX axis at a known position (say $z = (-10, 0)$). We place a_3 at various locations in the 2D plane and compute nr_3 for every position. The results are presented in Fig. 7. A point (x_0, y_0, z_0) on this graph should be read as: if anchor a_3 was placed at coordinates (x_0, y_0) in the 2D plane, the value of nr_3 is given by z_0.

Note that the noise resilience (nr_3) has a minimum of 0 in the case a_1, a_2 and a_3 are collinear (the distances $\overline{d}_3$ and $\overline{d}'_3$ are equal). nr_3 has a maximum of $\|z, z'\|$ in the case that a_3 is placed on the line (z, z') in one of the intervals $(-\infty, z)$ or (z', ∞). It is interesting to notice that it does not really matter where exactly in these two intervals a_3 is placed – the metric reaches its maximum for both segments.

The second observation is that noise-resilience metric includes the effects of the distance $\|z, z'\|$ in its definition. The larger this distance, the further away a_3 needs to be placed. In case z is the same as z', nr_3 is zero all over the 2D plane (meaning that $\overline{d}_1$ and $\overline{d}_2$ alone are enough for the node to compute its position).

In the following we explore the problem of determining where to best place three anchors in the 2D plane [12] from the perspective of the noise-resilience metric alone.

5.1 Single node localization

We place an unknown node in the origin of the 2D plane, and three anchors at random positions around it. We start an iterative procedure: we compute for each anchor where it should be placed if the positions of the node and the other two anchors were fixed and maximizing noise resilience would be the only criteria. Let us assume that anchor i is placed at position a_i and that it should be moved to a'_i. We associate a mass m with this anchor and define a force $F_i = k\|a_i - a'_i\|$ (the force vector is oriented from a_i to a'_i). We compute the F_i forces for each anchor and move the anchors under these forces towards the new positions. At the next iteration step we recompute the F_i forces and move the anchors again. We observe the equilibrium of this mass-spring system.

Recall that the nr_i metric is maximized for two disjoint line segments, hence, there are many options for the exact placement of a'_i point on these segments. In our experiment a'_i is chosen as the projection of a_i on the line determined by z and z', unless that projection is situated between z and z' in which case we select z as the position for a'_i.

Fig. 8 presents typical examples of such an experiment. The triangle shows the final position of the anchors. The lines connected to the triangle vertexes show the trajectories the anchors followed during the experiment.

The resulting anchor configuration is a triangle containing the node, but not necessarily *an equilateral triangle*. Indeed, from the explanation of the noise-resilience metric one can notice that the anchors will converge to a position where the node is situated in the intersection of the altitudes of the triangle – the orthocenter (the line formed by the node and an anchor a_i is orthogonal to the line formed by the other two anchors).

The trajectories and final placement of the anchors depends on the exact definition of the forces and the masses – non-linear forces and behavior in special cases as when an anchor position overlaps the position of the node could be considered in more detail. Nevertheless, the important aspect is that no matter where the three anchors converge, the final configuration will have the node in the orthocenter of the triangle defined by them.

5.2 Multiple nodes localization

The localization problem is strongly related to the deployment area of the nodes. Given a square deployment surface (say the space defined by $x \in [0, 1]$, $y \in [0, 1]$) and a random placement of multiple (say 200) nodes, we are interested in where to place three anchors such that the noise resilience is maximized with respect to all nodes.

Due to geometrical considerations, it is obvious that the noise-resilience metric can not take the maximum value for all the nodes at the same time. We apply the mass-spring approach previously described in the following way: at each iteration step, we compute the set of ideal positions for the anchor a_i taking every single node deployed into account. Let a_{im} be the mean value of all these values. We define the force $F_i = k\|a_i - a_{im}\|$ (the vector orientation is from a_i to a_{im}).

For *the same configuration of nodes*, we run the system with different anchor starting positions. Fig. 9 presents two examples of the results. It is interesting to notice that the anchors converge to different configurations (towards the boundaries of the deployment area) depending on their initial positions.

This experiment reveals another property of the proposed noise-resilience metric; it does not output a single configuration of anchors because it does not achieve its maximum in a single point. The fact that the metric is maximized as long as an anchor belongs to a certain interval introduces several possibilities of anchor configurations between which we cannot distinguish.

One of the conclusions we can draw is that geometry is the first step in solving the localization problem: a metric as noise resilience can provide a set of feasible anchor positions that minimizes the risk of flipping situations. A statistical analysis of the position estimator with respect to the specific type of noise added to the real distances should provide the second step in the localization algorithms – a metric helping to choose a specific anchor configuration from the given set.

6. TOWARDS AN EXPLANATION

We abstract the exact procedure of computing a position. We assume the coordinates of the n anchors a_i are known. We place a node at a position z. Let f be the function that translates a_i and z into a set of distances $\overline{d}_i$. Let f^{-1} denote the function through which a_i and $\overline{d}_i$ are mapped back into the position z. The function f^{-1} denotes the perfect one-hop distance-based localization algorithm running with noise-less data. In practice, exact distances are not available. We thus feed noisy measurements d_i into the function f^{-1} and receive a computed position $\tilde{z}$. The new distances between $\tilde{z}$ and a_i, written as $\tilde{d}_i$, slightly differ from d_i, compensating for the noise.

In the case of collinear anchors, given anchor positions a_i and distances $\overline{d}_i$, two positions z, z' can be computed (see Fig. 4). Note that a_i and $\overline{d}_i$ alone do not offer enough information to distinguish between the two cases, thus f^{-1} is undefined (a function associates only one output value to a given input). The default definition of f^{-1} leads to undefined behavior over the input domain, even when *the real distances* $\overline{d}_i$ are available. This is one of the reasons why CRB does not hold: f^{-1} is assumed always defined and equal to the real position of the node. In order to account for the flipping uncertainty, triggered by anchor geometry *and* by measurement noise as in Fig. 1(c), f^{-1} needs to be redefined to output a single value also in the case collinearity (or in the case of only one or two anchors being present).

Another observation we can make is that when the value of the noise exceeds the noise-resilience value for a geometrical structure, the localization algorithm will compute positions that can be part of multiple clusters rather then a single one (see Fig. 1(c)). There exists a trade-off between the amount of noise that can be applied to distance measurements and the noise-resilience factor of a given localization setup.

7. CONCLUSIONS AND FUTURE WORK

In this paper we showed that the one-hop distance-based localization mechanism has *geometry* as its foundation and not *measurement noise* as CRB assumes. The localization boundaries should thus be explored first from a geometrical perspective and then complemented by knowledge of the noise characteristics. We have supported this claim with a series of examples showing the limitations of the current approach.

We introduced a new metric (noise resilience) and explored the anchor deployment problem from its perspective. We showed that procedures for anchor placement can be derived solely from geometrical considerations. A statistical analysis on the measurement noise effect (such as a CRB technique) should complement this first step.

Based on this argumentation, we propose a radical change in the way in which the localization problem is to be addressed:

a. Basic concept: geometrical setup (positions of the anchors and of the node);
b. Theoretical steps: define f^{-1} mapping anchor positions and distances to an estimated position; determine the geometrical boundaries for maximum allowed errors;
c. Algorithm: from the formulation of geometrical boundaries determine the metric to be minimized to obtain a position (leading to a "geometric" lateration procedure);
d. Post processing: explore new metrics for the positioning error (Euclidean distance is considered the default one – it is nevertheless a one-dimensional metric that cannot express all the characteristics of a higher-dimensional phenomenon).

This description is also the base for our future work in which we wish to explore the trade-offs between geometrical setup (e.g. noise resilience) and amount of noise; as well as define a boundary under which noisy measurements will lead to a set of clustered positions. Our final target is to provide a clear formulation of the achievable boundaries of localization algorithms and to offer a new metric to be minimized taking the geometry of the setup and the measurement noise into account.

8. REFERENCES

[1] G. Mao, B. Fidan, and B. Anderson, "Wireless sensor network localization techniques," *Comput. Netw.*, vol. 51, no. 10, pp. 2529–2553, 2007.

[2] S. Gezici, "A survey on wireless position estimation," *Wirel. Pers. Commun.*, vol. 44, no. 3, pp. 263–282, 2008.

[3] N. Patwari and al., "Locating the nodes: cooperative localization in wireless sensor networks," *IEEE Signal Process. Mag.*, vol. 22, no. 4, pp. 54–69, 2005.

[4] L. Hu and D. Evans, "Localization for mobile sensor networks," in *Proc. MobiCom*, 2004, pp. 45–57.

[5] R. Bischoff and R. Wattenhofer, "Analyzing connectivity-based multi-hop ad-hoc positioning," in *Proc. PerCom*, 2004, pp. 165–174.

[6] D. Niculescu and B. Nath, "Ad hoc positioning system (aps)," in *Proc. GLOBECOM*, 2001, pp. 2926–2931.

[7] A. Savvides, W. Garber, R. Moses, and M. Srivastava, "An analysis of error inducing parameters in multihop sensor node localization," *IEEE Trans. Mobile Comput.*, vol. 4, no. 6, pp. 567–577, 2005.

[8] D. Torrieri, "Statistical theory of passive location systems," *IEEE Trans. Aerosp. Electron. Syst.*, vol. AES-20, no. 2, pp. 183–198, 1984.

[9] M. Spirito, "On the accuracy of cellular mobile station location estimation," *IEEE Trans. Veh. Technol.*, vol. 50, no. 3, pp. 674–685, 2001.

[10] J. Zhu, "Calculation of geometric dilution of precision," *IEEE Trans. Aerosp. Electron. Syst.*, vol. 28, no. 3, pp. 893–895, 1992.

[11] K. Langendoen and N. Reijers, "Distributed localization in wireless sensor networks: a quantitative comparison," *Comput. Netw.*, vol. 43, no. 4, pp. 499–518, 2003.

[12] N. Bulusu, J. Heidemann, and D. Estrin, "Adaptive beacon placement," in *Proc. ICDCS-21*, 2001.